# Prediction of Milling Forces by Integrating a Geometric and a Mechanistic Model

S. Abainia, M. Bey, N. Moussaoui and S. Gouasmia

***Abstract*— In milling processes, the prediction of cutting forces is of great importance for machining free form surfaces. Due to the continuous curvature variations of these surfaces, cutting forces are variable. The prediction of cutting forces helps to minimize tool deflections and vibrations in order to increases tool life, to avoid tool breakage and to obtain a good surface finish. The aim of this work is to predict the milling forces while finishing free form surfaces on 03-axis CNC milling machines using ball end milling tools by integrating a mechanistic cutting force model and a geometric model.**

***Index Terms*—Dexel, STL model, Free Form Surface, Cutting Forces, Mechanistic model**

## I. Introduction

IN manufacturing, the appropriate cutting conditions must be selected in order to reduce tool wear, tool deflections, vibrations and to have a stable machining and finally to obtain a good surface finish. When machining free form surfaces, contact regions between ball end mills/surface are variables which make cutting forces vary continuously along the tool path due to the continuous curvatures variation of these surfaces. This fact is considered by many researchers.

In [1], a model is developed to predict cutting forces applied to ball end mill by considering several parameters. In [2], the influence of dynamic radii, radial and axial depths on milling forces is studied. In [3], geometric and mechanistic milling models are integrated to predict cutting forces and feedrate scheduling for five-axis machining. In [4], a comparison is done between graphical mechanistic model with simulation method and experimental results. In [5], finite element method is used to substitute experimental works to predict the cutting forces. In [6], feedrate for three axis machining is selected by combining geometric and mechanistic models. In [7], an analytical milling force model is used to optimize cutting conditions.

The aim of this paper is to predict cutting forces applied on ball end mill tools for each tool position and for each tooth along tool path while finishing free form surfaces on three-axis CNC milling machines by integrating a geometric model using dexels and a mechanistic force model.

S. ABAINIA. Centre de Développement des Technologies Avancées (CDTA), Cité 20 Août 1956, BP N°17 Baba Hassen, Algiers, Algeria, (e-mail: s_abainia@yahoo.fr).

M. BEY. Centre de Développement des Technologies Avancées (CDTA), Cité 20 Août 1956, BP N°17 Baba Hassen, Algiers, Algeria, (e-mail: bey_mohamed@yahoo.com).

## II. Proposed Approach

The proposed approach contains five steps (Figure 1). The different steps are detailed in the following sub-sections.

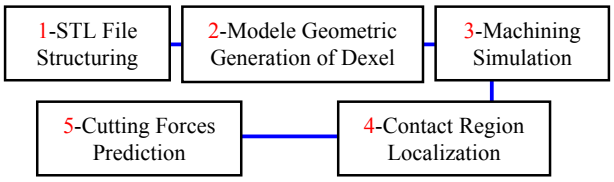


Fig. 1. Steps of the proposed approach.

### A. STL File Structuring

The STL model represents the outer skin of objects by a list of triangles, where their number and their size depend on the object geometry and the tolerances of approximation. Each triangle is defined by the components of its unit normal vector $\vec{N}$ oriented to the outside of the object and by the coordinates X, Y and Z of its vertices $P_1$, $P_2$ and $P_3$

### B. Generation of the Dexel Model

Dexels are used to approximate solid objects by material columns parallel to the Z-axis where their bases can be square or rectangular. Dexels are created from these steps:

- Cells creation : to accelerate the intersection calculus between triangles and dexels, two lists are created (Figure 2) :
  - Uniform grid of cells for grouping triangles entirely contained in one cell ;
  - Supplementary cell for grouping triangles belonging at least to two cells.

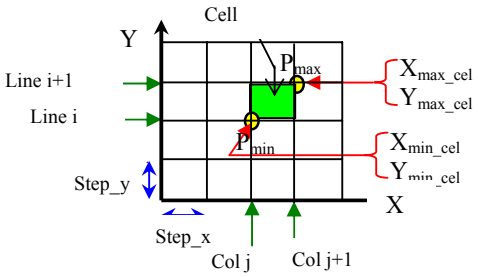


Fig. 2. Cells grid creation.

- Dexels creation: the center of each dexel ($X_0$, $Y_0$) and its two extremums points along the Z-axis ($Z_{min}$ and $Z_{max}$) to define its height H are calculated (Figure 3).

ISBN: 978-988-19252-2-0
ISSN: 2078-0958 (Print); ISSN: 2078-0966 (Online)

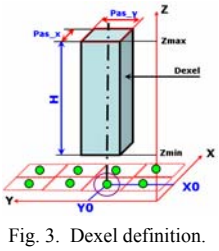


Fig. 3. Dexel definition.

- *Dexel center calculus*: the center of each dexel is calculated from the dimensions and the coordinates of the extremums points of the raw part using the specified steps along X-axis (pas_x) and Y-axis (pas_y).
- *Height dexels calculus*: the dexel height is calculated from the determination of the extremums points intersection between the vertical line passing by its center with the set of triangles.

### C. Machining simulation

This step permits to simulate the finishing machining using ball end mills for any machining strategy (Parallel Planes, Isoparametric, Z-Constant, etc.). it passes by:

- Addition of the stock allowance to each dexel with the condition that the top face of the dexel must not exceeds the superior face of the raw part (Figure 4).

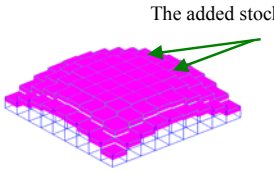


Fig. 4. Addition of the stock allowance.

- Dexel-sphere intersection: the contact regions for ball end mills are determined from the calculation of the intersection points between ball end mills and dexels for each tool position. This necessitates the following steps:

For a tool position :

- Recuperate the coordinates of the sphere center C(xc,yc, zc) and its radius R;
- Determine the limits of the sphere envelope;
- Determine the dexels having intersections with the sphere envelope;
- Determine the intersection points between the sphere and the vertical lines passing by dexels centers ($X_0$, $Y_0$) from the following equations system :

$$\begin{cases} (X-xc)^2+(Y-yc)^2+(Z-zc)^2=R^2 \\ X=X_0 \\ Y=Y_0 \end{cases} \quad (1)$$

Three cases must be considered:

- One intersection point: this point is retained (Figure. 5.a)
- Two intersection points: the lower point is retained (Figure. 5.b).
- No intersection points (Figure. 5.c).

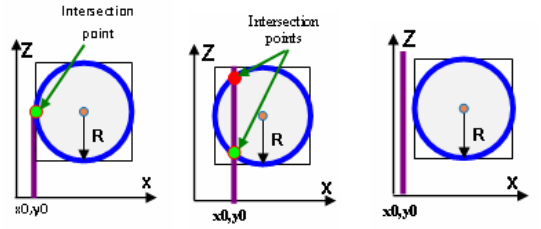


a. One point. b. Two points. c. No intersection.

Fig. 5. Intersection cases of vertical straight line and a sphere.

- Dexels height update: after calculating the intersection points, an update of the height dexels is necessary by considering the two following cases:
  - *Case 1*: if ($Z_{material} > Z_{intersection}$), then an update must be done. So, $Z_{material} = Z_{intersection}$ (Figure. 6.a).
  - *Case 2*: if ($Z_{material} < Z_{intersection}$), then no update is required (Figure. 6.b).


a. An update is necessary. b. No any update.

Fig. 6. Update of dexels height.

### D. Contact region localization

The determination of the contact regions between cutting tools and surfaces for a tool position passes by these steps:

- *Cutting tool segmentation*: consists in subdividing the active part (spherical part) of the ball end mill into a set of discs with the same thickness for each tool position. The limited active part by this slicing is determined from $Z_{min}$ and $Z_{max}$ of the intersection points list (Figure. 7). Once disc thickness is specified, disc center, disc radius and limits ($z_{min\_disc}$ and $z_{max\_disc}$) for each disc are determined.

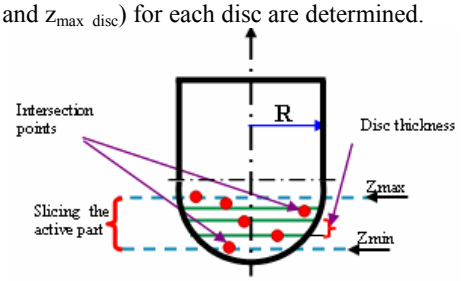


Fig. 7. Segmentation of the active part.

- *Affectation of points to discs*: the intersection points associated to each disc are determined based on the Z coordinate of the intersection points and the limits of the disc ($z_{min\_disc}$ and $z_{max\_disc}$). Next, the position angle for each point is calculated according to the X-axis (Figure. 8). This angle is between 0° and 360°.

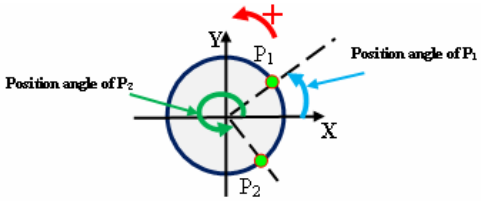


Fig. 8. Position angle of points.

ISBN: 978-988-19252-2-0
ISSN: 2078-0958 (Print); ISSN: 2078-0966 (Online)

✓ *Creation of the contact regions for each disc*: after the affectation of the intersection points to discs, the different contact regions for each disc and the entrance angle and the exit angle associated to each region are calculated. The determination of these parameters passes by these steps (Figure. 9) :

- ☆ Sorting the intersection points based on their position angles;
- ☆ Affectation of intersection points to contact regions :
  - ❖ Run through the intersection points list:
    - ⇨ Test the difference of the position angle between two consecutive points to a predefined angle θ:
      - ♦ If this difference is less than $\theta$, then the two points belong to the same region;
      - ♦ If this difference is greater than θ, then a new region is created and the second point is affected to this new region;
- ☆ For each contact region:
  - ✓ The entrance angle $\phi_{ent}$ is equal to the position angle of the first point of this region.
  - ✓ The exit angle $\phi_{exit}$ is equal to the position angle of the last point of this region.

The predefined angle θ is a constant that depends on the dexel steps "*pas_x*" and "*pas_y*", disc radius "*R*" and a real coefficient "*Coef*". This angle is given by:

$$\theta = \frac{Max(pas\_x, pas\_y)}{R}.Coef \qquad (2)$$

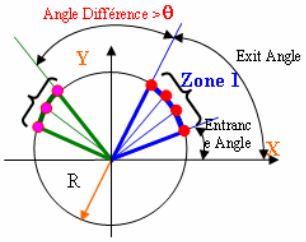


Fig. 9. Determination of the contact regions for a disc.

### *E. Cutting forces prediction*

The proposed approach uses a mechanistic force model to predict the cutting forces for each tool position along the tool path in three axis machining. For a given point on the ball end mill, the differential components cutting forces (tangential $dF_t$, radial $dF_r$ and axial $dF_a$) in a local cartesian system linked to the cutting tool (Figure. 10) corresponding to an infinitesimal element edge length of the cutting tool is given by [6]:

$$\begin{cases} dF_t = K_{tc}(h_a)^{-p1} h(\phi,z)dS \\ dF_r = K_{rc}(h_a)^{-p2} h(\phi,z)dS \\ dF_a = K_{ac}(h_a)^{-p3} h(\phi,z)dS \end{cases} \qquad (3)$$

With:

$h_a$ : average thickness of the chip.

$h(\phi, z)$ : instantaneous thickness of the chip.

dS : edge cutting length.

$K_{tc}$, $K_{rc}$, $K_{ac}$, $p_1$, $p_2$ and $p_3$: constants determined by experimental tests. They depend on edge geometry, tool and workpiece material.

The cutting forces components $dF_x$, $dF_y$ and $dF_z$ in cartesian system are given by:

$$\begin{bmatrix} dF_x \\ dF_y \\ dF_z \end{bmatrix} = \begin{bmatrix} -\sin\phi\sin\kappa & -\cos\phi & -\sin\phi\cos\kappa \\ -\cos\phi\sin\kappa & \sin\phi & -\cos\phi\sin\kappa \\ -\cos\kappa & 0 & -\sin\kappa \end{bmatrix} \begin{bmatrix} dF_t \\ dF_r \\ dF_a \end{bmatrix} \qquad (4)$$

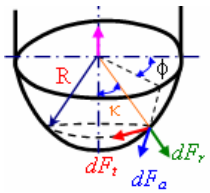


Fig. 10. Cutting forces for a ball end mill.

With ϕ is the angular position of a tool point.

An elementary disc is defined by its radius "R(z)" and its positioning angle "κ" given by (Figure 11):

$$\kappa = arcsin((R(z))/R) \qquad (5)$$

Where R is the tool radius.

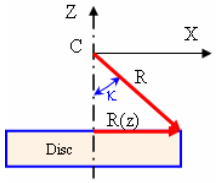


Fig. 11. Elementary disc parameters.

In the cartesian system (X, Y, Z), the cutting forces are predicted using the following parameters:

➢ Average chip thickness for a disc given by:

$$h_a = f_t.n_t \sum_{i=1}^{ni} \frac{(\cos\phi_{sort} - \cos\phi_{ent})\cos\theta_2 \cos\beta}{\phi_{ent} - \phi_{sort}} \qquad (6)$$

With :

$\theta_2$: angular position of an elementary disc (Figure. 12).

$n_i$ : number of regions of a disc.

β : angle between the displacement vector *D* for two consecutives positions and the X-axis (Figure. 12).

$f_t$ : tooth feedrate (mm/tooth).

$n_t$: teeth number.

Tooth feedrate is given by the following formula:

$$ft = \frac{f}{nt \times \Omega} \qquad (7)$$

With: f : feedrate of the cutting tool (mm/min).

Ω : spindle speed (tr/min).

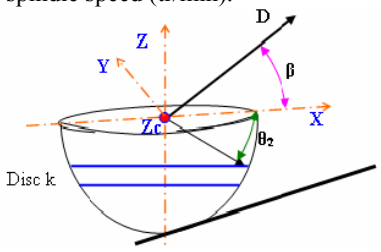


Fig. 12. Geometric parameters of a disc.

ISBN: 978-988-19252-2-0
ISSN: 2078-0958 (Print); ISSN: 2078-0966 (Online)

- Instantaneous chip thickness given by [6] :

$$h(\phi,z)=\frac{f_t\left[\cos\theta_2\sin\phi\cos\beta-\sin\theta_2\sin\beta\right]}{n_t\Omega} \quad (8)$$

- Cutting edge length given by (Figure. 13):

$$\begin{cases} dS = R.d\theta = R.(\theta_2 - \theta_1) \\ \theta_1 = arcsin((Zc - Z_{max\_disq})/R)) \\ \theta_2 = arcsin((Zc - Z_{min\_disq})/R)) \end{cases} \quad (9)$$

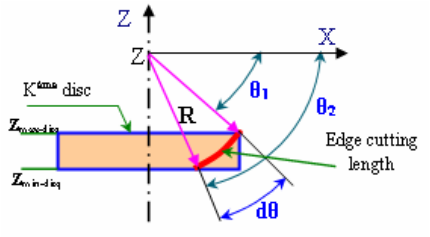


Fig. 13. Geometric parameters of a disc.

The prediction of the cutting forces for a tool position passes by the following steps:

1. Calculus of the cutting forces for a contact region.
2. Calculus of the cutting forces for a disc.
3. Calculus of the resultant cutting forces.

- For each disc:
  - For each contact region:
    - Subdivide each contact region into a set of points with a constant angular increment (Figure 14).
    - For each point corresponding to a position angle ϕ:
      - Calculate the angles $\theta_2$ and β.
      - Calculate the average chip thickness $h_a$.
      - Calculate the instantaneous chip thickness $h(\phi,z)$.
      - Calculate the cutting edge length dS.
      - Calculate the differentials cutting forces $dF_t$, $dF_r$ and $dF_a$.
      - Calculate the angle κ.
      - Calculate the cutting forces $dF_x$, $dF_y$ and $dF_z$.
    - Sum all the cutting forces to obtain the cutting force for the considered region.
      - ✓ Sum all the cutting forces to obtain the cutting force on each disc.
      - ✓ Sum all the cutting forces for all discs to obtain the resultant cutting force.

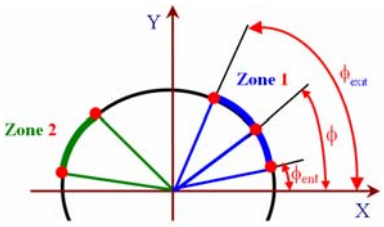


Fig. 14. Position angle of point for a disc.

To predict the cutting forces in three directions X, Y and Z applied on each tooth, the helix angle is considered. For this, the necessary steps are:

- For a given complete rotation of the cutting tool:
  - Determine the contact regions limits.
  - Segment the active part of the tool into a set of discs with equal heights (Figure.15);
  - For the elementary top disc;
    - Create a set of points with a given angular step.
    - For each point:
      - Calculate the corresponding point for the tooth number k by:

$$\phi_p=\phi_{ref}+(k-1).\frac{2\pi}{N_t} \quad (10)$$

Where $\phi_{ref}$ is taken equal to 0°.

- Determine the corresponding contact regions;
- Calculate the instantaneous thickness;
- Calculate the average thickness;
- Calculate the differential forces dFt, dFa and dFr (Figure.16).
  - Calculate the forces Fx, Fy and Fz applied on each tooth.

  - For the other discs:
    - Calculate the corresponding points by:

$$\phi_k(z)=\phi_{ref}+(k-1)\frac{2\pi}{n_t}-\frac{\tan\beta}{R}z \quad (11)$$

Where β is the helix angle.

- Determine the corresponding contact regions;
- Calculate the instantaneous thickness;
- Calculate the average thickness;
- Calculate the differential forces dFt, dFa and dFr (Figure.16).
- Calculate the forces Fx, Fy and Fz applied on each tooth.

- ☆ Calculate all cutting forces applied on the ball end mill.

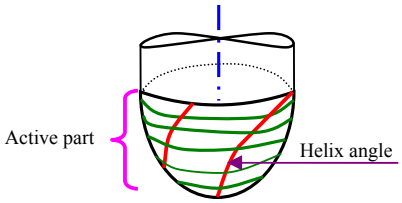


Fig. 15. Segmentation of the active part.

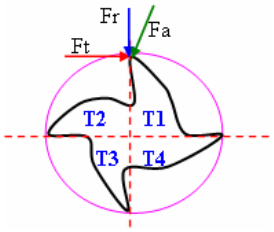


Fig. 16. Cross-sections of 4 flute end mill.

## III. Results

The proposed approach is implemented in object-oriented software under Windows using C++ Builder and the graphical library OpenGL [8]. The validation of this approach is performed on an STL model of a part generated from a CAD model (Figure. 17). The dimensions of the raw part are 140mm×160.7mm×51.3mm. The tool path is generated using a ball end mill of a radius equal to 8 mm (Figure. 17.c).

ISBN: 978-988-19252-2-0
ISSN: 2078-0958 (Print); ISSN: 2078-0966 (Online)

a. CAD Model.

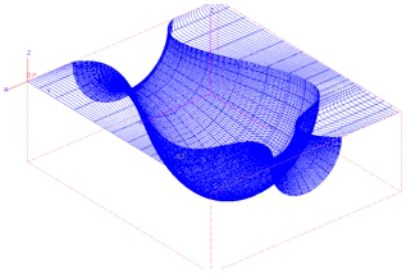

b. STL Model.

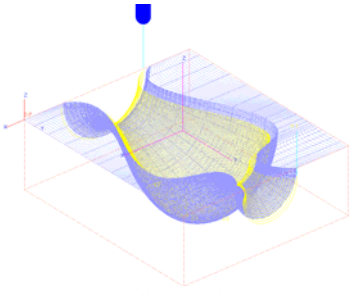

c. Machining tool path.

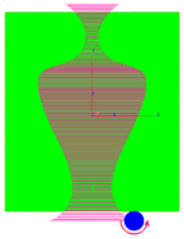

d. Top view.

Fig. 17. CAD and STL models and tool path.

The dexel model of the CAD part is generated from a step equal to 0.2 mm along X-axis and Y-axis (Figure 18).

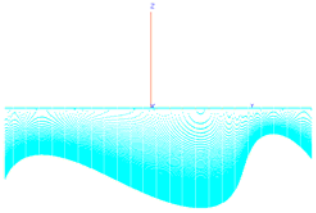

a. Intersection points between vertical lines and triangles in YZ plane.

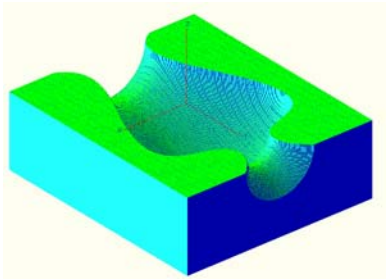

b. Dexel Model.

Fig. 18. Creation of the dexel model.

To simulate the machining, the stock allowance is fixed equal to 1 mm (Figure. 19). Figure 20 shows the tool while machining simulation.

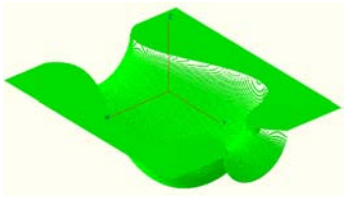

Fig. 19. Stock allowance.

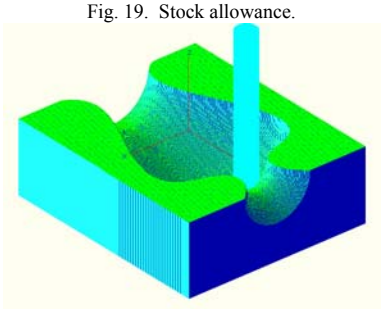

Fig.20. Machining simulation.

During simulation, the intersection points between dexels and the sphere of the ball end mill for each tool position are calculated. Figure 21 shows the intersection points for the tool position number 64619.

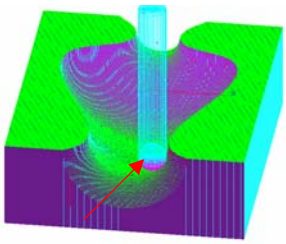

a. Tool position number 64619.

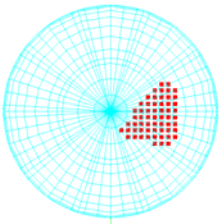

b. Intersection points.

Fig. 21. Results for a specific tool position.

Next, the contact regions of each disc are determined. To predict the cutting forces, the fixed parameters are:

- Number of teeth=4;
- Angular increment=1°;
- Spindle speed= 1500 tr/min;
- Feedrate=500 mm/min.

Table 1 gives the values of the constants used in the mechanistic cutting force model.

| Ktc | Krc | Kac | P1 | P2 | P3 |
|---|---|---|---|---|---|
| 535 | 125 | 256 | 0.24 | 0.26 | 0.25 |

Table 1. Values of the experimental constants [3].

Figures from 22 to 27 shows the different results related to the cutting force components for each tool position number.

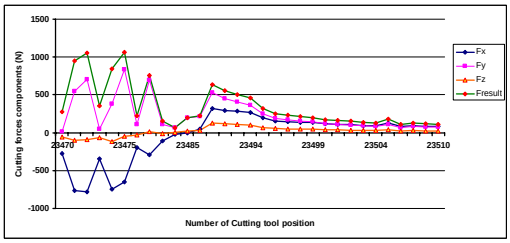


Fig. 22. Cutting force components variations.

ISBN: 978-988-19252-2-0
ISSN: 2078-0958 (Print); ISSN: 2078-0966 (Online)

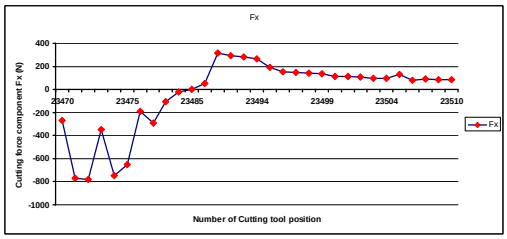


Fig. 23. Cutting force component Fx variations.

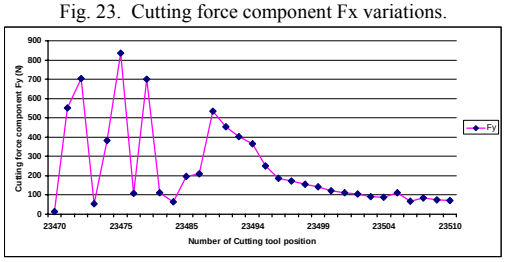


Fig. 24. Cutting force component Fy variations.

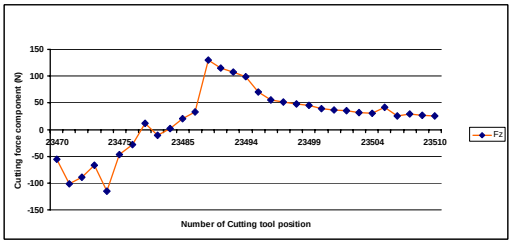


Fig. 25. Cutting force component Fz variations.

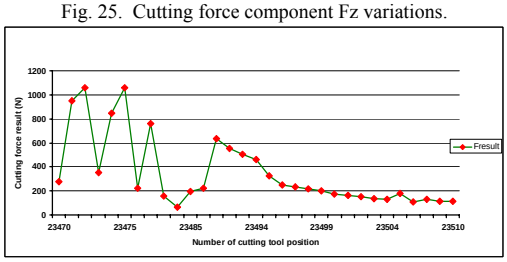


Fig. 26. Cutting force result variations.

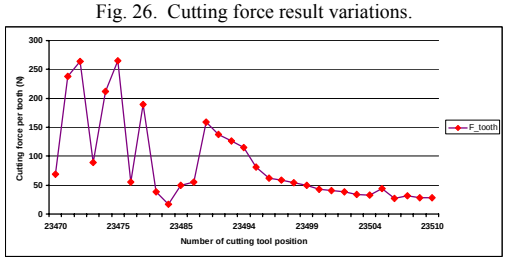


Fig. 27. Variations of cutting force average per tooth.

Many remarks can be extricated from the different graphs:

- For each cutting tool position, Fy is more greater than Fx and Fz also Fz is greater than Fx.
- The cutting force Fx vary in the interval [-271 N, 729 N].
- The cutting force Fy vary in the interval [0 N-836 N].
- The cutting force Fz vary in the interval [-115 N, 130 N]
- The cutting force resultant vary in the interval [0 N, 1059 N]

The abrupt fluctuations of the cutting forces along the tool path is due to the continuous suddenly variations of the surface curvatures.

Figure 28 shows the variations of the cutting force per tooth versus the tool position.

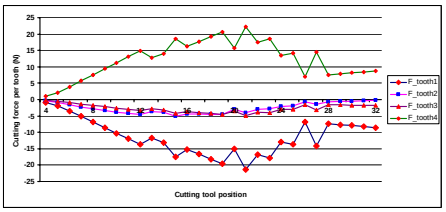


Fig. 28 Variations of cutting forces per tooth.

The results show that the cutting forces vary continuously from a tooth to another. This variation is more influenced by the part curvatures.

## IV. Conclusion

In this paper, an approach is proposed and implemented for predicting the cutting forces applied on the end ball mill during the finishing of free form surfaces defined by their STL model on 3-axis CNC milling machines. In this approach, the dexels elements are used to approximate the solid model of the part, machining simulation is used for determining the effective contact regions between ball end mills and surfaces and a mechanistic force model is used to predict cutting forces for each tool position along any machining tool path.

The results show the influence of the surfaces curvatures variations on the contact region between ball end mills and surfaces and consequently on the cutting forces. This can help to anticipate the force peak at any position along the tool path and therefore to avoid the breakage of the cutting tool and the machine elements.

In perspective, the determination of the optimal cutting conditions permitting to have a stable machining and a good surface finish will be considered.

## References

[1] Ismail Lazoglu, "Sculpture surface machining: a generalized model of ball-end milling force system," *International Journal of Machine Tools & Manufacture*, 43 453–462, Manufacturing, Automation & Research Centre, Koc, University Istanbul, Turkey, 2003.

[2] Wen-Hsiang Lai, "Modeling of Cutting Forces in End Milling Operations," University of Kansas, Tamkang *Journal of Science and Engineering*, Vol. 3, No. 1, pp. 15-22, 2000.

[3] Liqiang Zhang, Jingchun Feng, Yuhan Wang & Ming Chen, "Chen, Feedrate scheduling strategy for free-form surface machining through an integrated geometric and mechanistic model," *Int Journ Adv Manuf Technol*, 40:1191–1201, DOI 10.1007/s00170-008-1424-6, 2009.

[4] D. Roth, F. Ismail, S. Bedi, "Mechanistic modelling of the milling process using complex tool geometry," *Int Journ Adv Manuf Technol* 25: 140–144, DOI 10.1007/s00170-003-1853-1, 2005.

[5] O. Gonzalo, H. Jauregi, L. G. Uriarte & L. N. López de Lacalle, "Prediction of specific force coefficients from a FEM cutting model," *Int Journ Adv Manuf Technol*, DOI 10.1007/s00170-008-1717-9.

[6] B. K. Fussell R. B. Jerard J. G, Hemmett, "Robust Feedrate Selection for 3-Axis NC Machining Using Discrete Models," University of New Hampshire, *Journal of Manufacturing Science and Engineering* MAY 2001, Vol. 123 / 221, DOI: 10.1115/1.1365398.

[7] E. Budak, "Analytical models for high performance milling. Part I: Cutting forces, structural deformations and tolerance integrity," *International Journal of Machine Tools & Manufacture* 46 1478–1488, Sabanci University, Istanbul, Turkey, 2006.

[8] M. Dixon et M. Lima, "OpenGL programming guide," Addisson-Wesley Publishing Company, 1997.

ISBN: 978-988-19252-2-0
ISSN: 2078-0958 (Print); ISSN: 2078-0966 (Online)